

From 2D to 3D: A Facile and Effective Procedure for Fabrication of Planar CH₃NH₃PbI₃ Perovskite Solar Cells

Yu Zhang, Fengzhu Li, Ke-Jian Jiang,* Jin-Hua Huang, Huijia Wang, Haochen Fan, Pengcheng Wang, Cai-Ming Liu,* Li-Peng Zhang and YanLin Song*

Experimental Procedures

Materials. Unless stated otherwise, all materials were purchased from Sigma Aldrich and used as received. Ethylamine, methylammonium iodide was purchased from Xi'an Poly. Light Tech. Corp., and Spiro-MeOTAD was purchased from Merck KGaA.

Fabrication of single crystal (n-C₃H₇NH₃)₆Pb₄I₁₄: 5 g propylamine was added dropwise to a 57 % aqueous HI solution (40 ml) under ice-bath. Then, 8.8 g PbI₂ powder (10 mM) was added under stirring. The reaction was carried under constant magnetic stirring at 80 °C under oil bath for 1 h. After that, the stirring was then discontinued, and the heating was turned off and let to cool down until room temperature, during which time yellow crystals formed. The crystals were isolated by suction filtration and thoroughly dried under reduced pressure. The as-synthesized yellow crystals show a rod-shaped structure with a diameter of about 1 mm and a length of 2~4 mm.

X-ray Crystallography: A single crystal with dimensions 0.093 × 0.081 × 0.056 mm³ of **1** was picked out to mount on a Bruker SMART APEX-CCD diffractometer with Mo-K α radiation ($\lambda = 0.71073$ Å) for data collection at 113 K. Empirical absorption corrections from φ and ω scan were applied. Cell parameters were obtained by the global refinement of the positions of all collected reflections. The structure was solved by direct methods and refined by a full matrix least-squares technique based on F² using the SHELX-2014 program package. All non-hydrogen atoms were refined anisotropically, and all hydrogen atoms were refined as riding atoms. The crystal data and data collection and refinement parameters for complex **1** are listed in **Table S3**. CCDC 1854533 contains the supplementary crystallographic data, which can be obtained free of charge from the Cambridge Crystallographic Data Centre via www.ccdc.cam.ac.uk/data_request/cif.

Solar cells fabrication. Fluorine-doped SnO₂ (FTO) substrates were ultrasonically washed with deionized water, acetone, and isopropanol for 30 min successively. After drying, the cleaned FTO glass was treated by UV-ozone (UVO) for 15 min then used immediately for device fabrication. 0.15 M and 0.3 M titanium diisopropoxide bis(acetylacetonate) were spin-coated on the clean substrate at 3,000 r.p.m. for 30 s, then it was dried at 125 °C for 10 min and sintered at 500 °C for 60 min. The substrate was immersed in 40 mM TiCl₄ aqueous solutions at 70 °C for 30 min and washed with distilled water and ethanol, followed by annealing at 500 °C for 30 min in air to form a compact layer of TiO₂. After the substrate was allowed to cool, a layer of PCBM (20 mg/ml in 1,2-dichlorobenzene) was deposited via spin coating at 3000 rpm for 30 s, followed by annealing at 100 °C for 1 h. For the perovskite precursor solution, 1g (n-C₃H₇NH₃)₆Pb₄I₁₄ crystal was dissolved in 1 mL dimethylformamide (DMF) and stirred at 50 °C for 24 h. The resulting solution was coated onto the FTO/compact TiO₂/PCBM substrate by a consecutive two-step spin-coating process at 1,000 and 5,000 r.p.m for 5 and 30 s, respectively, without requiring solvent treatment during the coating. After drying at 80 °C for 5 min, the precursor films were subsequently subjected to cation-displacement reaction in methylamine (MA) gas, where the MA gas was produced by reacting methylammonium chloride with sodium hydroxide with CaO as desiccant in a closed container. The reaction was carried out at 100 °C for 5 min in a fume cupboard. After the cation exchange reaction, the perovskite film was taken out and immediately transferred to the N₂-filled glovebox, annealing at 150 °C for 10 min to remove the excessive MAI. A hole-transporting layer of spiro-OMeTAD was deposited by spin-coating at 4,000 r.p.m. for 30 s in a glovebox. 1 mL spiroOMeTAD/chlorobenzene (80 mg/mL) solution was employed with addition of 17 μ L lithium bis(trifluoromethanesulfonyl)imide (Li-TFSI)/acetonitrile (520 mg/mL) and 28 μ L of 4-*tert*-butyl

pyridine. Finally, an 80 nm Au electrode was deposited via thermal evaporation at a constant rate of 0.01 nm/s.

Characterization. The X-ray diffraction (XRD) patterns of the prepared films were recorded using an X-ray diffractometer (Rigaku, D/MAX RINT-2500) with Cu K radiation ($= 1.54 \text{ \AA}$) at a speed of 2° min^{-1} . The absorption spectra were collected using a UV/Vis spectrometer (SHIMADZU, UV-1800 UV/Vis Spectrophotometer) in the wavelength range of 300–850 nm. The surface and cross-sectional morphologies of the films as well as the thicknesses were analyzed by using a JEM-7500F field-emission scanning electron microscope (SEM). X-ray photoelectron spectroscopy (XPS) were performed on the Thermo Scientific ESCA Lab 250Xi using 200 W monochromated Al $K\alpha$ radiation, and 500 μm X-ray spot was used for XPS analysis. Typically the hydrocarbon C 1s line at 284.8 eV from adventitious carbon is used for energy referencing. Steady-state photoluminescence (PL) was measured using Edinburgh FLS980 system with an excitation at 640 nm. Time-resolved photoluminescence decays were measured with a time-correlated single-photon counting system, and the excitation wavelength was 500 nm with a power of $\sim 25 \mu\text{W}$ on a spot size of 0.02 mm^2 . The decay curve was fitted using a double exponential model. Element compositions were determined using Thermo Finnigan elemental analyzer (Flash EA1112). The nuclear magnetic resonance (NMR) spectra were measured on an Avance III 400MHz NMR spectrometer. Current–voltage characteristics were recorded by applying an external potential bias to the cell while recording the generated photocurrent with a Keithley model 2400 digital source meter. The light source was a 300 W collimated xenon lamp (Newport) calibrated with the light intensity to 100 mW cm^{-2} under AM 1.5G solar light conditions by a certified silicon solar cell. The J–V curve was recorded by the reverse scans with a rate of 100 mV s^{-1} . The active area was determined by metal shadow mask. The external quantum efficiency (EQE) for solar cells was performed using a commercial setup (PV-25 DYE, JASCO). A 300 W Xenon lamp was employed as a light source for the generation of a monochromatic beam. EQE spectra were recorded using monochromatic light without white light bias. Calibrations were performed with a standard silicon photodiode. EQE is defined by $\text{EQE}(\lambda) = hcJ_{sc}/e4I$, where h is Planck's constant, c is the speed of light in a vacuum, e is the electronic charge, λ is the wavelength in meters (m), J_{sc} is the short-circuit photocurrent density (mA cm^{-2}), and 4 is the incident radiation flux (W m^2). The space charge limited current (SCLC) measurement through Keithley source table (Keithley 2400, USA).

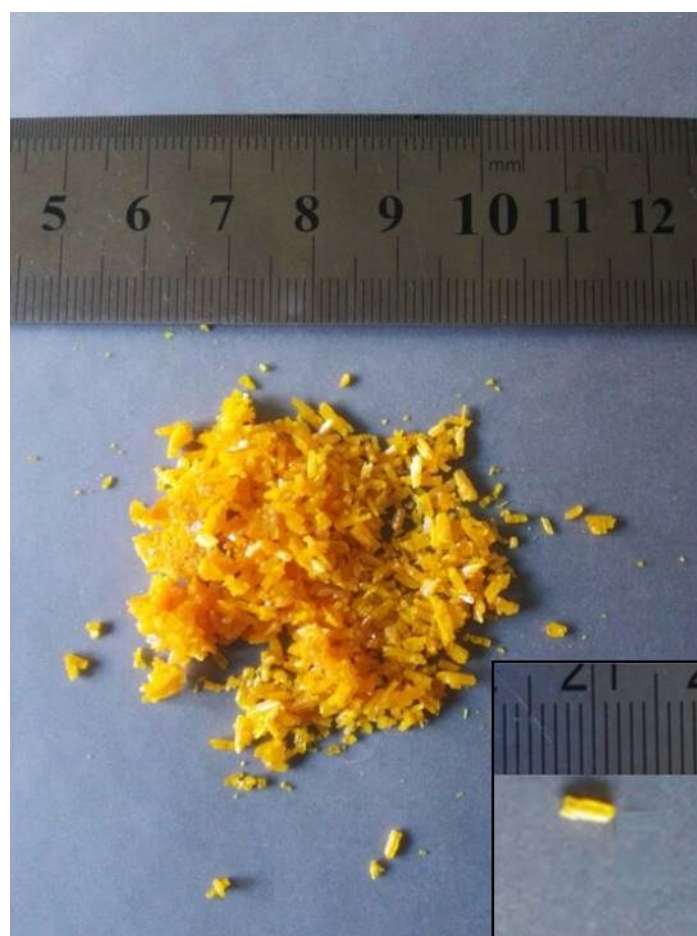


Figure S1 Photographs of single crystal complex **1** $(n\text{-C}_3\text{H}_7\text{NH}_3)_6\text{Pb}_4\text{I}_{14}$

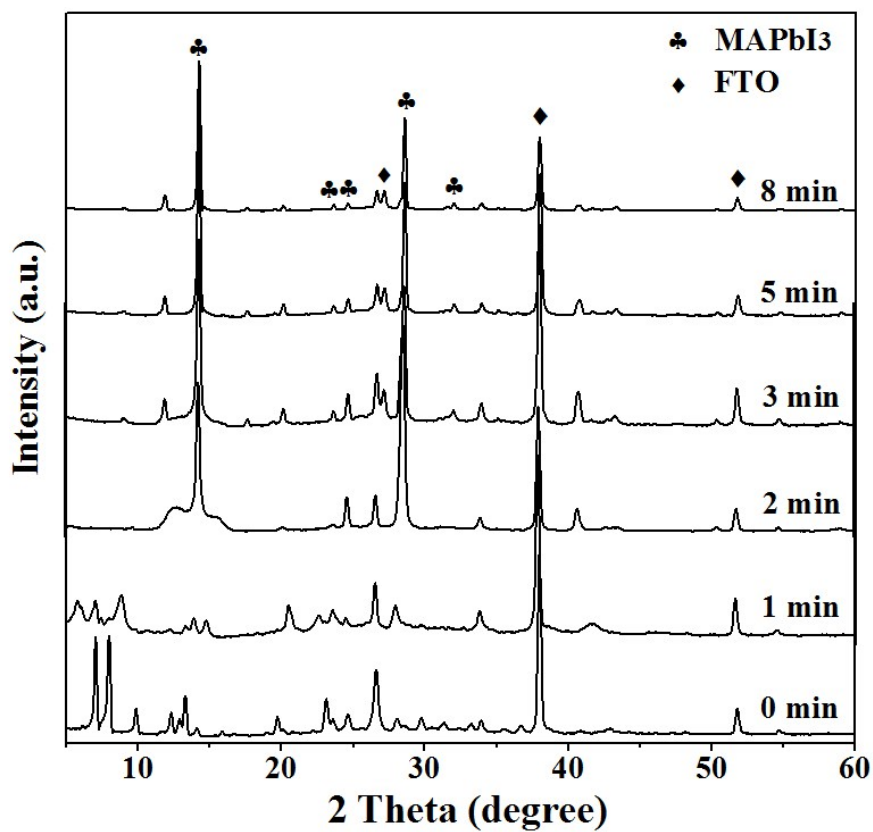


Figure S2 X-ray diffraction (XRD) spectra of the as-converted CH₃NH₃PbI₃ film via the cation-displacement at 100 °C for 0, 1, 2, 3, 5 and 8 min.

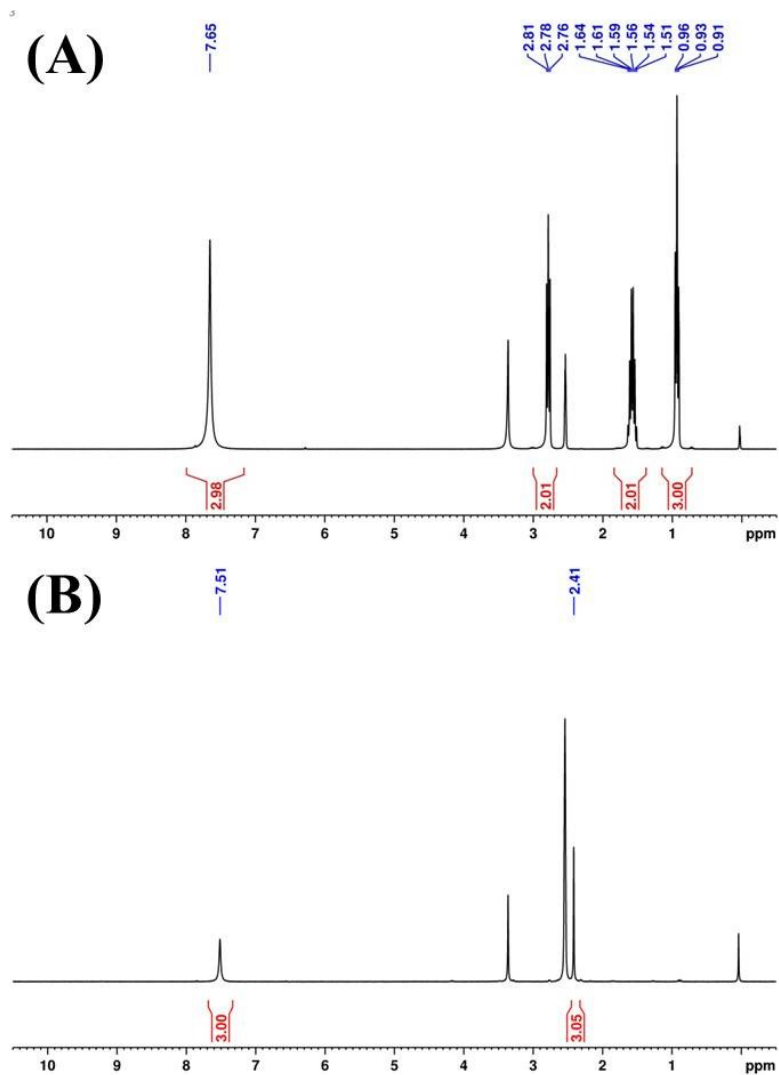


Figure S3 ^1H NMR spectra of the 2D single crystal $(n\text{-C}_3\text{H}_7\text{NH}_3)_6\text{Pb}_4\text{I}_{14}$ and the converted MAPbI_3 after MA treatment and annealing process (A) $(n\text{-C}_3\text{H}_7\text{NH}_3)_6\text{Pb}_4\text{I}_{14}$, ^1H NMR (300 MHz, d_6 -DMSO) δ 7.65 (3H, s, NH_3), 2.76-2.81 (2H, t, CH_2), 1.51-1.64 (2H, m, CH_2), 0.91-0.96 (2H, t, CH_3). (B) MAPbI_3 ($\text{CH}_3\text{NH}_3\text{PbI}_3$) ^1H NMR (300 MHz, d_6 -DMSO) δ 7.51(3H, s, NH_3), 2.41 (3H, d, CH_3).

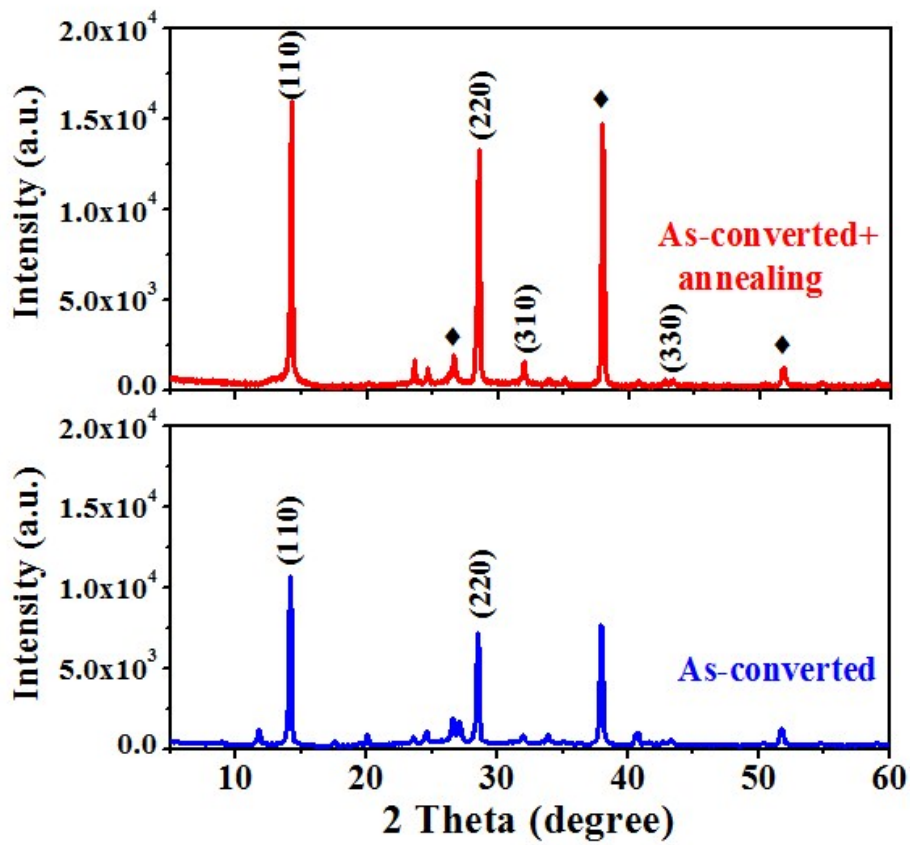


Figure S4 X-ray diffraction (XRD) spectra of the as-converted $\text{CH}_3\text{NH}_3\text{PbI}_3$ film via the cation-displacement at 100 °C for 5 min, and the as-converted $\text{CH}_3\text{NH}_3\text{PbI}_3$ with annealing at 150 °C for 10 min. ◆ denotes FTO peaks of the substrates

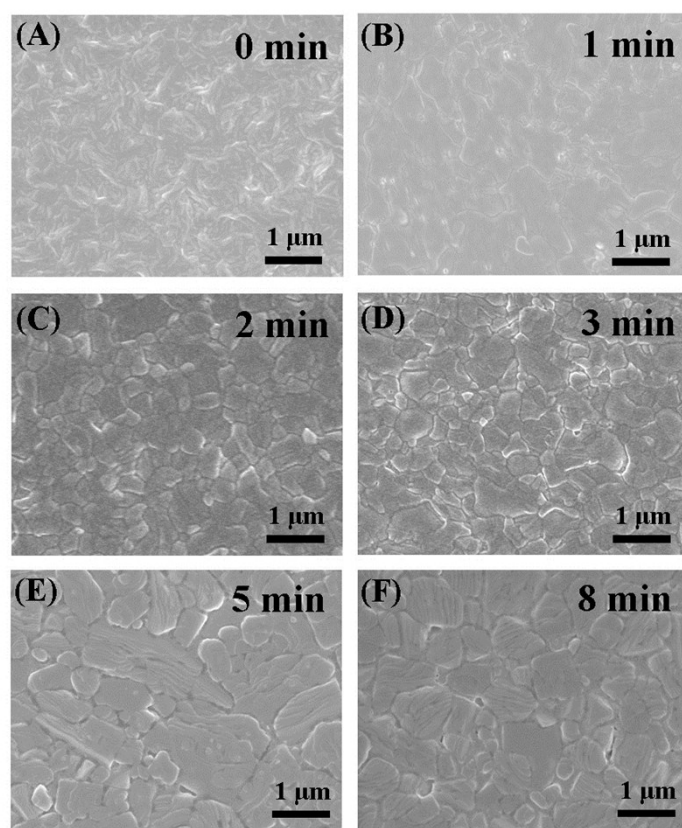


Figure S5 SEM micrographs of as-converted $\text{CH}_3\text{NH}_3\text{PbI}_3$ film via the cation-displacement at 100 °C for 0, 1, 2, 3, 5 and 8 min.

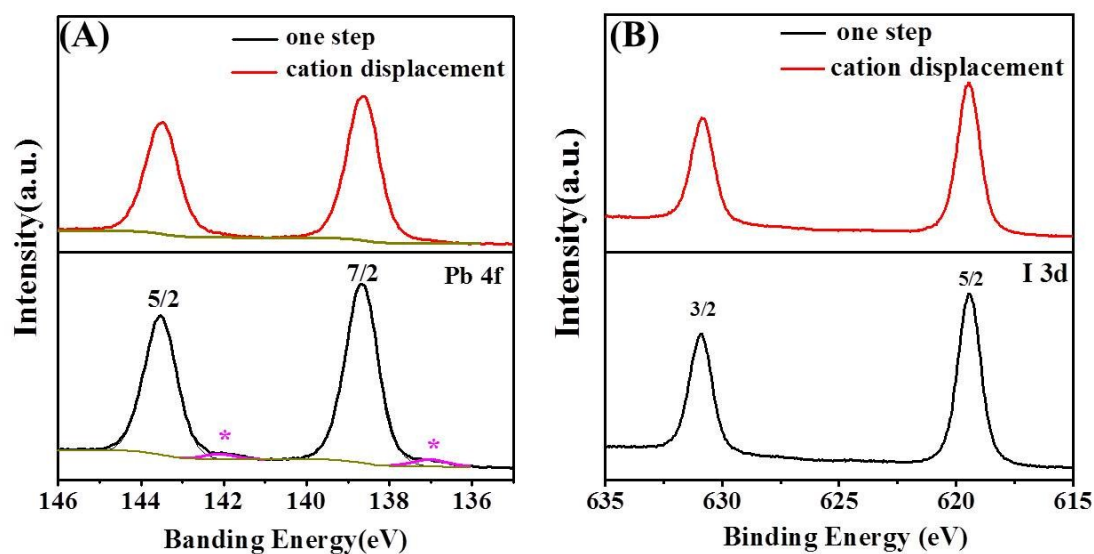


Figure S6 The high resolution XPS spectra of **A)** Pb 4f and **B)** I 3d core-level spectra of the perovskite film with cation-displacement and one-step method. The spectra of Pb (**A**) both show two spin-orbit splitting peaks at 138.7 and 143.6 eV with a separation of 4.90 eV, which are corresponding to Pb 4f_{7/2} and Pb 4f_{5/2} binding state, respectively. The above binding energies are well consistent with reported values for Pb²⁺ bonded to Pb-I in CH₃NH₃PbI₃. However, the film made by one-step method shows a couple of small peaks at around 137.0 and 141.9 eV assigned to the presence of unsaturated metallic Pb (Pb⁰). The I 3d spectra (**B**) both present a single I 3d_{5/2} peak at 619.5 eV with a spin-orbit splitting of 11.4 eV to I 3d_{3/2} at 630.9 eV, which proves that all the I are bonded with Pb without any I₂ in perovskite film. These findings suggest that a little Pb²⁺ is reduced to metallic Pb⁰ during one-step method, and these metallic lead species in the perovskite films are likely to act as recombination centres and shorten the PL lifetime.

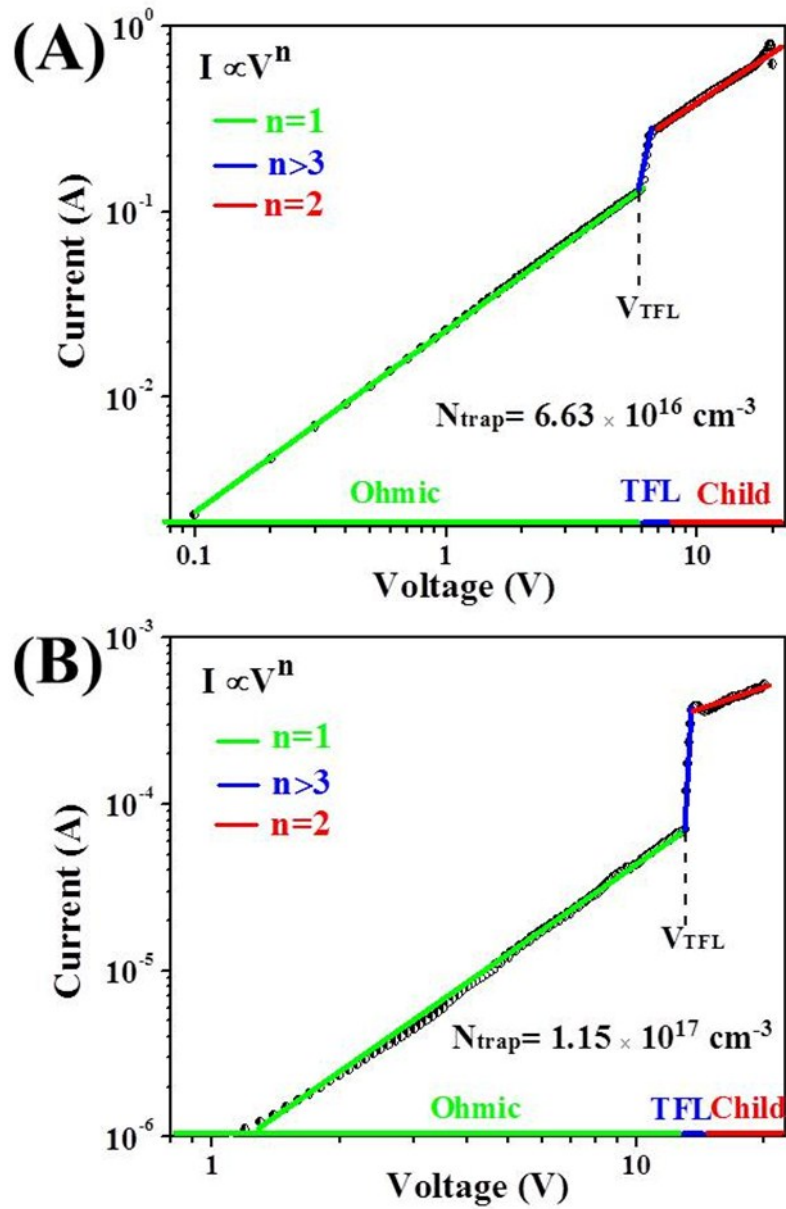


Figure S7 Current-voltage characteristics of device with FTO/perovskite/Au configuration for estimating the defect density in perovskite films prepared by cation-displacement (A) and one-step method (B).

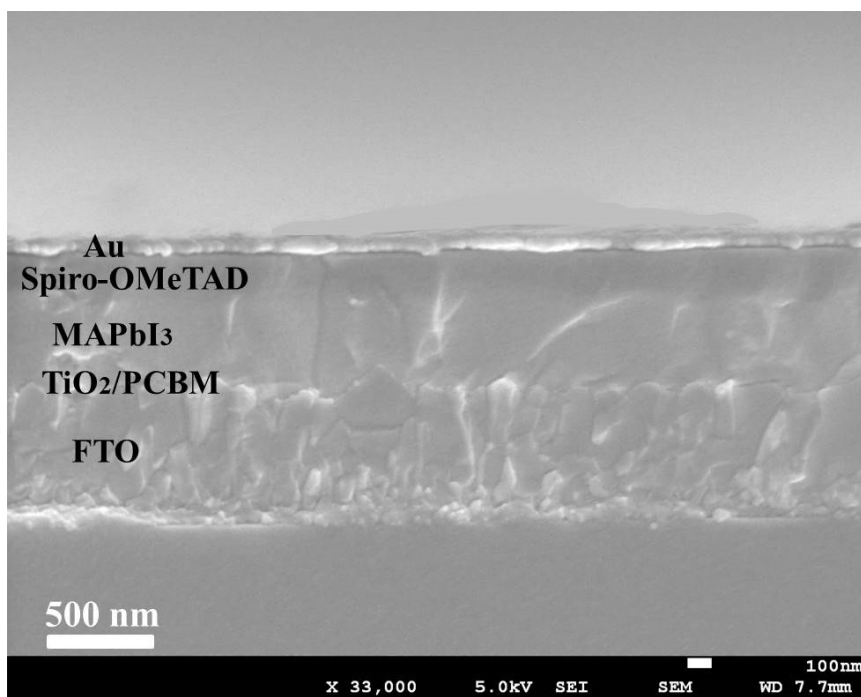


Figure S8 Cross-sectional SEM image of a complete solar cell by cation-displacement method.

Table S1 Theoretical and measured element analysis data for the samples, **A)** Complex **1**, **B)** the as-converted $\text{CH}_3\text{NH}_3\text{PbI}_3$ film via the cation-displacement at 100 °C for 5 min, **C)** the as-converted $\text{CH}_3\text{NH}_3\text{PbI}_3$ with annealing at 150 °C for 10 min.

	Element Content / %	C	H	N
A	Measured	7.32	2.01	2.80
	Theoretical	7.28	2.02	2.83
B	Measured	2.59	1.28	3.02
	Theoretical	2.57	1.29	3.00
C	Measured	1.95	0.96	2.27
	Theoretical	1.94	0.97	2.26

Table S2 Fitting decay times of perovskite films prepared by one-step and cation-displacement method.

Fluorescent Lifetime/ ns	τ_1	τ_2	τ
One step	67.4	359.3	287.5
Cation displacement	166.7	1431.7	1186.4

**Table S3 Crystal data and structure refinement for (n-
C₃H₇NH₃)₆Pb₄I₁₄.**

Identification code	(CH ₃ CH ₂ CH ₂ NH ₃) ₆ Pb ₄ I ₁₄
Empirical formula	C ₁₈ H ₆₀ I ₁₄ N ₆ Pb ₄
Formula weight	2966.08
Temperature/K	113.15
Crystal system	monoclinic
Space group	P2 ₁
a/Å	8.7287(17)
b/Å	22.221(4)
c/Å	15.080(3)
α/°	90
β/°	91.16(3)
γ/°	90
Volume/Å ³	2924.5(10)
Z	2
ρ _{calc} /cm ³	3.368
μ/mm ⁻¹	18.888
F(000)	2560.0
Crystal size/mm ³	0.093 × 0.081 × 0.056
Radiation	MoKα (λ = 0.71073)
2θ range for data collection/°	2.702 to 55.05
Index ranges	-11 ≤ h ≤ 11, -28 ≤ k ≤ 28, 0 ≤ l ≤ 19
Reflections collected	13373
Independent reflections	13373 [R _{sigma} = 0.0657]
Data/restraints/parameters	13373/175/392
Goodness-of-fit on F ²	1.092
Final R indexes [I ≥ 2σ (I)]	R ₁ = 0.0800, wR ₂ = 0.2118
Final R indexes [all data]	R ₁ = 0.0826, wR ₂ = 0.2140
Largest diff. peak/hole / e Å ⁻³	9.11/-8.58
Flack parameter	0.038(4)